*Refereed Proceedings*

*The 13th International Conference on Fluidization - New Paradigm in Fluidization Engineering*

Engineering Conferences International *Year* 2010

# A NOVEL CHEMICAL LOOPING COMBUSTION PROCESS: PRESSURE DROP AND SOLID CIRCULATION RATE MODELLING

Ali Hoteit* Yazdanpanah Mohammad-Mahdi† Forret Ann‡
Delebarre Arnaud** Gauthier Thierry††

*IFP-Lyon, Ali.Hoteit@ifp.fr
†IFP-Lyon
‡IFP-Lyon
**Université Henri Poincaré, Nancy, France
††IFP-Lyon

# A NOVEL CHEMICAL LOOPING COMBUSTION PROCESS: PRESSURE DROP AND SOLID CIRCULATION RATE MODELLING

Yazdanpanah Mohammad-Mahdi[1], Hoteit Ali[1*], Forret Ann[1], Delebarre Arnaud[2], Gauthier Thierry[1]
[1] IFP-Lyon, Rond-point de l'échangeur de Solaize BP 3 - 69360 Solaize – France
T: + 33 (0)4 78 02 55 71, F: +33 (0)4 78 02 20 08,
*E: Ali.Hoteit@ifp.fr
[2] Université Henri Poincaré, Nancy, France

## ABSTRACT

Experimental results from a cold flow unit of a novel chemical looping combustion configuration are presented in this paper. The system employs a non-mechanical l-valve to control solid flow rate and uses loop-seals to minimize gas leakage. A model was developed to predict solid flow rate and pressure variation in different elements of the system. The developed model was able to well predict solid flow rate within an error range of 10% for a wide solid flux range of 70 – 150 kg/m².s. Sensibility of the solid flow rate was analyzed for different operating parameters by aid of the model. Particles diameter demonstrated to have highest impact on the solid flow rate. Particles density and solid inventory in the reactor were affecting the solid flow rate with less impact. Pressure variation loop over the first section of the system was finally presented for three different solid flow rate.

## INTRODUCTION

Global warming and its consequent effect on climate change is one of the major overriding environmental, social and economic threats facing mankind. Carbon capture and storage (CCS) is considered as an midterm solution to the stated problem, permitting reduction of $CO_2$ emission with minimum change in current energy sources. Chemical Looping Combustion (CLC) is a kind of oxy-combustion process involving indirect combustion of fuel with in situ oxygen separation and without any direct contact between air and fuel. The resulting flue gas is a ready to capture $CO_2$ stream diluted with water vapor which can be easily condensed out. Accordingly, CLC can provide an effective solution for clean consumption of fossil fuels with low cost capture of $CO_2$ and maximum energy production efficiency comparable to conventional power generation stations.

## Chemical Looping Combustion

Various designs have already been proposed for CLC studies. These could be classified into two general categories, interconnected fluidized bed designs (1-10) and innovative processes (11-14). In the first category, the most common design is based on the conventional circulating fluidized bed (CFB) systems with addition of a second reactor as fuel reactor (1-3). In these systems a low velocity bubbling fluidized bed reactor is devoted to fuel reaction and a high velocity riser is considered as air reaction. The advantageous of this design is the fact that due to its similarity with conventional CFB combustion process, it is best adopted with existing power generation units and its phenomena are well studied to date. Studies reveal the fact that solid flow control can be achieved in this configuration (4-5), however it is a function of gas flow in the reactors and solid inventory in each reactor, i.e. it could not be adjusted independently from other parameters of fluidization. In order to improve solid circulation control and achieve proper residence time in the reactors different modified designs are developed to date. Forero et al. (6) have added a bubbling fluidized bed as AR just below the riser. De Diego et al. (7) have also used an bubbling fluidized bed as AR while separating the riser and the AR using a loop-seal. Kolbitsch et al. (8) have developed concept of Dual Circulating Fluidized Bed (DCFB) where FR is in turbulent regime forming a second loop inside the overall system. They have accordingly achieved to control the solid flow rate just based on the aeration rate in AR, independent from the gas rate in FR. Keronberger B. et al. (9) have developed an alternative design, two compartment fluidized bed reactor, with simplified design resulting in smaller installations requirement and lower cost. Son et al. (10) have proposed an annular fluidized bed CLC reactor in order to provide sufficient reaction time and optimize heat transfer between the reactors. Alstom Power Inc. (11) has developed a novel system based on the calcium sufide which includes an additional cycle of calcination. More innovative design have been also proposed as: packed bed CLC (12), Packed bed membrane assisted chemical looping reactor (13) and rotating bed reactor (14).

IFP and TOTAL have started a R&D collaboration project on CLC. As a part of the project, a novel design based on the interconnected bubbling fluidized bed concept was developed at IFP to build a 10 $kW_{th}$ pilot plant. The main concern was to insure an independent solid flow control, similar to what is found in some already mature fluidized bed catalytic processes such as FCC (15). In order to study hydrodynamic and mechanical behavior of the system a cold physical prototype was constructed with similar geometrical dimensions as the hot model (Fig 1). This paper presents modeling results based on the experimental findings of the cold CLC prototype.

## MATERIALS AND METHODS

The cold prototype was constructed with transparent plexiglass which helps in visual observation during experimentations and facilitates modifications. The system (Fig 1) is composed of two interconnected bubbling fluidized bed reactors, R1 and R2 with circular cross section of 0.1 m and height of 1 m. Bubbling beds are used to ensure sufficient contact time between solid and gas/air to achieve optimum reaction conversion. Beside, this will result in higher flexibility of the system and permits use of various oxygen carriers with different oxidation and reduction reaction rates. Gases are injected at the bottom of the reactors through perforated plates. Reactors

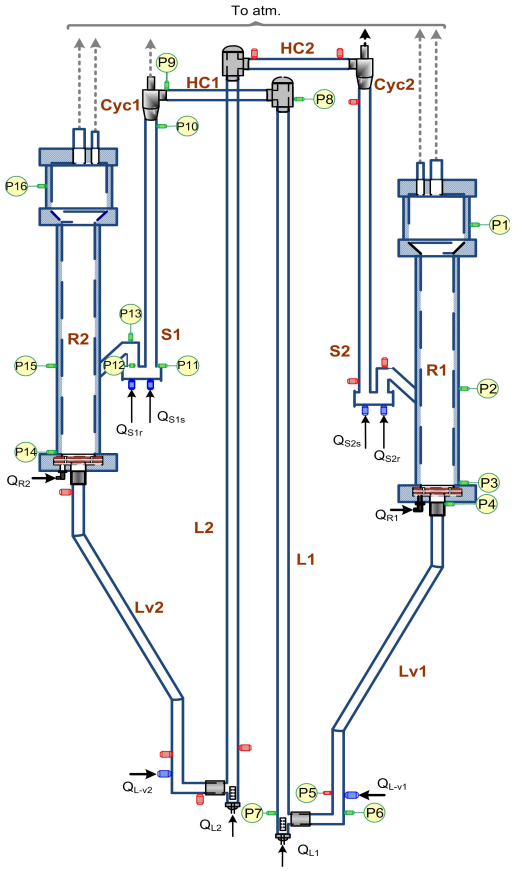


**Figure 1: Scheme of the CLC cold flow prototype ,Gas injection and pressure measurement taps are indicated .**

cross section increases at top in order to reduce gas velocity and trap the entrained solids back to the reactor.

In order to achieve a maximum flexibility of the system it was important to control solid flow independent from other operating variables. The best solid flow control can be achieved by use of mechanical valves adapted to solid flow; however high temperatures in CLC process limits use of mechanical valves. Consequently, non-mechanical l-valves were employed for this purpose. As illustrated in Fig.1, l-valves are composed of hybrid stand-pipes with inclined sections in order to convey the solids horizontally. Solids at the exit of the l-valves are transported through a vertical lift followed by a horizontal conveying line. Solid gas separation is performed in a cyclone where separated solids are lead to a loop-seal located in the bottom of the cyclone dipleg. Loop-seals were employed to ensure gas tightness of the reactors.

Experiments were carried out in ambient conditions using air as fluidizing gas in each reactor. This paper presents results for sand particles with 334 µm average diameter, 2650 kg/m$^3$ solid density, 1440 kg/m$^3$ of bulk density, and 0.068 m/ of measured minimum fluidization velocity.

Pressure drops were measured by digital pressure transducers and were automatically registered on a computer with adjustable frequency. Different pressure taps were located on the installation to permit proper measurement of pressure variation. Location of pressure taps is illustrated in Fig 1. Compressed air is supplied from a compressed air network with constant pressure. Gas inflow for l-valves and loop-seals are controlled using specific mass flow rate controllers connected to a computer for data collection. Gas flow into the lifts and reactors are controlled with manual valves and flow rates are measured using rotameters with constant pressure.

## Solid Flow Rate Measurement

Solid flow rate measurement was carried out using batch solid flow between the reactors. A constant aeration was applied to the l-valve. By measuring circulated solid per unit of time, average solid flow rate was measured. Instantaneous solid flow rate was also calculated using the slop of the curve representing the evolution of pressure drop along the fluidized bed to measure bed level as:

$$W_s = \frac{dM_{s,R}}{dt} = \frac{A_R}{g} \cdot \frac{dP_R}{dt} \qquad (1)$$

This was measured for different aeration rates in the l-valve. One example is given on Figure 2. Measuring the pressure drop for a 2 m section of lift in fully developed flow regime provided a linear relation between lift pressure drop and solid flow rate (Fig. 3). The results were then used to calculate solid flow rate during steady state operation .

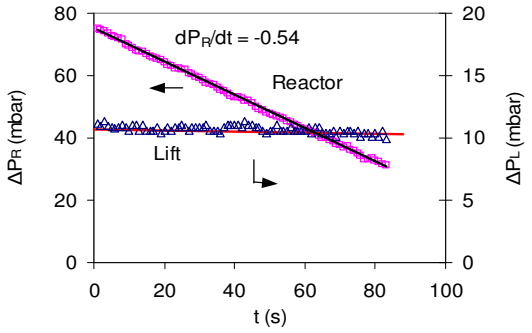


**Figure 2: Pressure drop in reactor and lift for constant aeration in the l-valve in a batch process.**

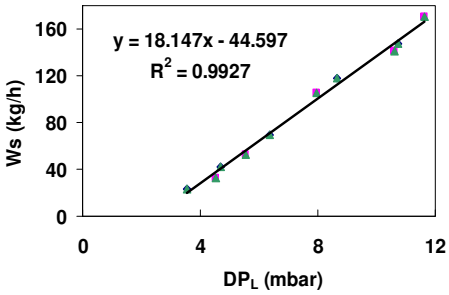


**Figure 3: Solid flow rate versus pressure drop in the lift ($U_{g,L}$ = 6.8).**

## MODELLING THEORY

In a stable solid circulation operation, pressure is balanced over solid circulation loop. The CLC system, as illustrated in Fig.1, is composed of two identical conveying lines between the 2 reactors. Therefore the same pressure balance methodology will apply for both lines. The pressure loops from atmospheric pressure in the gas exit above the first reactor to the atmospheric pressure exit in the second reactor is:

$$\Delta P_{R1} + \Delta P_{lv,v} + \Delta P_{lv,A-H} + \Delta P_L + \Delta P_{Tb} + \Delta P_{HC} + \Delta P_{Cyc,s} + \Delta P_{ls} + \Delta P_{DR2} = 0 \quad (2)$$

Since the cyclone on top of the lift has a gas exit connected to the atmosphere, equation 1 could be broken into two parts. Then first split including l-valve is:

$$\Sigma P_{lv} = \Delta P_{R1} + \Delta P_{lv,v} + \Delta P_{lv,A-H} + \Delta P_L + \Delta P_{Tb} + \Delta P_{HC} + \Delta P_{Cys,g} = 0 \quad (3)$$

Where ΔP is positive if pressure increases along the element and is negative if pressure decreases with reference positive direction is solid flow direction. A similar equation can be derived to develop pressure balance around the loop seal. If fluidized beds and cyclone outlets are operated at a different pressure, then an additional pressure difference term could be included in equations (2) and (3) to generalize the pressure balance.

Solid flow rate in the CLC system is controlled in the l-valve where total quantity of the gases passing through the horizontal section ($Q_{lv,H}$) determines the solid flow rate. The quantity of $Q_{lv,H}$ depends on the gas injected into the valve, $Q_{lv}$, and the gas flow in the standpipe ($Q_{lv,v}$).Therefore: $Q_{lv,H} = Q_{lv} \pm Q_{lv,v}$, where gas flow rate in the standpipe could be either upwards (positive sign) or downwards (negative sign) and is taken into account by: $\delta_{lv} = \pm Q_{lv,v}/Q_{lv}$. The gas flow amount and direction flowing in the standpipe will adjust to satisfy pressure balance equation (3) and therefore will depend on solid flow rate, but also upon operating conditions imposed such as bed level and pressure for instance.

A model was derived to calculate solid flow in the loop as a function of L-valve aeration and imposed operating conditions. An iterative computation method was

developed : knowing aeration rate into the l-valve, an initial value of 0 is set for the gas fraction factor ($\delta_{lv}$). Solid flow rate is then calculated using the horizontal solid flow rate correlation. Pressure drop in different sections of the system are then calculated based on the solid flow rate and given aeration rates into the system. Sum of the pressure drops across the first section of the transport line ($\Sigma P_{lv}$) is then calculated using equation 3. If $\Sigma P_{lv}$ is equal to zero, the results are considered as final results. Otherwise $\delta_{lv}$ is increased by an incremental value. This is continued till pressure drop is balanced over the loop.

Pressure drop in each section of the loop have to be calculated in order to complete pressure balance equations. Different simple correlations were used to describe in each section and are listed in Table 1.

**Table 1: Pressure drop and flow correlation used in the model for different sections.**

| Element | Pressure drop | Ref. |
|---|---|---|
| **Reactor**(P3-P1) | $\Delta P_R = M_R g / A_R = \rho(1-\varepsilon_R) g H_R$ | |
| **L-valve: Standpipe** (P5-P4) | $\Delta P_{lv,v} = -\Delta P_{R1} + \Delta P_{lv,H} + \Delta P_L + \Delta P_{Tb} + \Delta P_{HC} + \Delta P_{Cyc,g} + \Delta P_{piping}$<br>$\frac{\Delta P}{L} = 150.\frac{\mu_f v_r}{(\phi.d_s)^2}.\frac{(1-\varepsilon)^2}{\varepsilon^2} + 1.75.\frac{\rho_f v_r^{\,2}}{\phi.d_s}.\frac{(1-\varepsilon)}{\varepsilon}$<br>$v_r = v_s - v_g = \frac{U_{lv,vs}}{\varepsilon_{sp}} - \frac{U_{lv,vg}}{(1-\varepsilon_{sp})}$ | (16) |
| **L-valve: Horizontal** (P5-P7) | $\frac{\Delta P_{lv,A-H}}{L_{lv,H}} = 0.0844\frac{G_s^{\,0.137}}{\rho_b^{\,0.131} d_p^{\,0.64}}$<br>$\frac{G_s}{D_{lv}} = 2465\frac{U_{lv}}{U_{mf}} - 4763$ | modified from (17)<br>modified from (18) |
| **Lift** (P7-P8)<br>**Horizontal Conveying and T-Bend** (P8-P9) | $\frac{\Delta P_L}{L} = g.(1-\varepsilon).\rho_s + g\varepsilon\rho_g + \frac{2 f_s v_s^{\,2}(1-\varepsilon)\rho_s}{D} + \frac{2 f_g v_g^{\,2}\varepsilon\rho_g}{D} + \frac{\Delta P_{acc}}{L}$<br>$\frac{\Delta P_{HC}}{L} = \frac{2 f_s v_s^{\,2}(1-\varepsilon)\rho_s}{D} + \frac{2 f_g v_g^{\,2}\varepsilon\rho_g}{D} + \frac{\Delta P_{acc}}{L}$<br>$f_g = 0.0791\,\mathrm{Re}^{-0.25} \quad for \quad 3\times10^3 < \mathrm{Re} < 10^5$<br>$f_g = 0.0008 + 0.0552\,\mathrm{Re}^{-0.237} \quad for \quad 10^5 < \mathrm{Re} < 10^8$<br>$f_s = 0.0285\frac{\sqrt{g.D_P}}{v_p}$<br>$\Delta P_{acc} = 0.5\rho_g v_g^2 + kG_s v_s$ | (19)<br>(20)<br>(21) |
| **Cyclone** (P9-Patm) | $\Delta P_{Cyc,g} = \Delta P_{(f-i)g} + \Delta P_{(f-i)p} + \Delta P_{bf} + \Delta P_{rg} + \Delta P_o$ | (22) |

## RESULTS AND DISCUSSIONS

### Solid Circulation Control

Solid flow rate in the current installations is controlled by the l-valves aeration flow rate. It is known that solid flow rate in a l-valve is controlled by the quantity of the gas passing thought the horizontal section of the valve ($Q_{lv\text{-}H}$). However $Q_{lv\text{-}H}$ depends not only on the aeration rate into the l-valve but also to the gas flow in the vertical part of the l-valve above the aeration point (standpipe) (16). The gas flow rate in this section is determined by pressure drop developed across the standpipe

which depends on the overall pressure drop of the system and is calculated as shown in Table 1. In order to demonstrate this phenomenon in the l-valve, pressure drop variation in the standpipe of the l-valve is plotted during a batch experiment while solid inventory in the reactor R1 was emptied for a constant aeration rate in the l-valve (Fig 4).

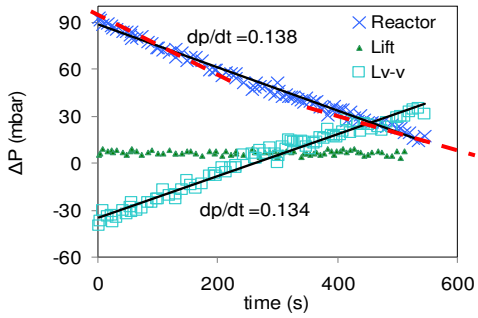


**Figure 4 : Pressure drop evolution in the standpipe of the l-valve for a batch solid circulation from R1 to R2 with $Q_{lv}$ = 0.08 $Nm^3/h$, and $G_s$ = 49 kg/m².s.**

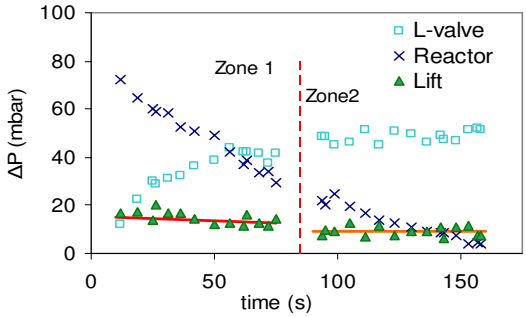


**Figure 5: Pressure drop evolution in the standpipe of the l-valve for a batch solid circulation from R1 to R2 with $Q_{lv}$ = 0.18 $Nm^3/h$, $G_s$ = 196 kg/m².s in zone 1 and 98 kg/m².s in zone 2 (right).**

As illustrated in Fig 4, pressure variation in the standpipe follows exactly the pressure variation of the reactor but in an opposite way. Reduction of pressure drop in the reactor (due to smaller inventory) increases the pressure drop in the standpipe of the l-valve to adjust the pressure balance around the circulation loop. Higher pressure drop across the standpipe reduces the gas flow rate through the standpipe. Accordingly $Q_{lv,H}$ reduces, resulting in solid flow reduction. This is illustrated in Fig 4 where solid flux in the L-valve varied from 60 kg/m².s in the period 0-100s to 40 kg/m².s in the period 430-530s.

Pressure across the standpipe can only increase until a limit which is fluidization of the l-valve. Thereafter pressure drop remains constant. In these conditions however, solid flow rate decreases due to formation of gas bubbles which increases the voidage and decreases the solid quantity in the valve. This limit is well demonstrated in Fig 5 where solid flux drops suddenly from 196 kg/m².s to 98 kg/m².s in the first zone of the graph.

## Model Validation

Model results in predicting solid flow rate in the circulation loop and pressure variation in the different elements of the circuit are illustrated in Fig 6 and Fig 7. Model prediction demonstrated good agreement with experimental results. Solid flow rate predictions remain well in an interval of 10 % error and pressure drop is properly calculated.
Sensitivity of the solid flow rate was analyzed for variation of particles diameter ($d_s$), density ($\rho_s$) and solid inventory of the reactor ($M_R$) using the model. The solid flow rate is highly sensitive to variation of particle diameter. Solids with lower diameter result in considerably higher solid flow rate. Increase in solid density raises the flow rate approximately by the same order. Solid inventory however shows less effect (compared to $d_s$ and $\rho_s$) on the flow rate with a variation of solid flow rate of 0.25 times of $M_R$ change. To validate sensibility prediction of model to solid inventory, the experimental results of Fig 4 were simulated with the model for identical operating

conditions. The same solid flux variation in the L-valve was found from 66 to 44 kg/m².s, i.e. 33%. This demonstrates that the model is well able to predict this phenomenon.

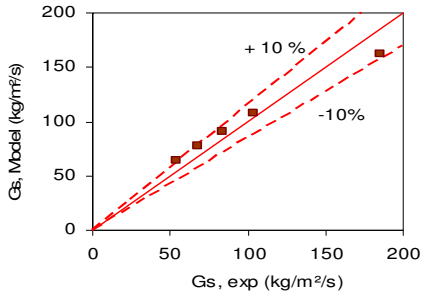


**Figure 6: Solid flow rate prediction by model versus the experimental results.**

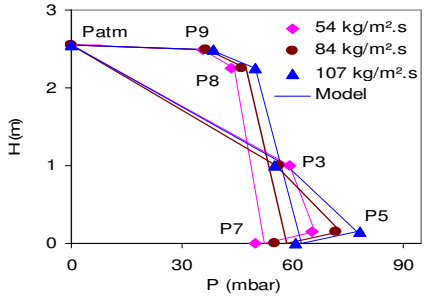


**Figure 7: Model prediction of pressure evolution for different heights in the prototype.**

**Table 2: Solid flow rate sensitivity analysis of the model parameters.**

| Parameter | Reference value | Variation (%) | Sensitivity (%) |
|---|---|---|---|
| $d_s$ | 321 µm | ± 10 | ± 21 % |
| $\rho_s$ | 2650 kg/h | ± 10 | ± 9 % |
| $M_R$ | 5.2 kg | ± 20 | ± 6 % |

## CONCLUSION

A novel design for process of chemical looping combustion is discussed in this paper. Solid circulation and pressure drop variation in a cold prototype is studied. L-valves are used to control solid flow rate in the system, permitting wide range control of solid flow regardless of gas velocities in the reactors. A model was developed based on the concept of overall pressure balance. Model predictions demonstrate good agreement with experimental results obtained from the cold prototype. Sensibility analyses were carried out using the model. It was found that the flow is mostly sensitive to variation of particle properties (diameter and density) and inventory of the solid in the reactor.

## NOMENCLATURE

**List of symbols**

A: Area of reactor, m².
$D_p$ : pipe diameter, m.
$d_s$ : solid particles size, m.
$f_g$: friction factor of gas flow
$f_s$: friction factor of solid flow
$G_s$: solid flux, kg/m².s
$H_R$: solid height in the reactor, m.
M: Mass of solid inventory, kg.
Q: gas flow rate, $Nm^3/h$.
t : time, s.
U: superficial velocity, m/s.
v: interstitial velocity, m/s.
$W_s$: Solid flow rate, kg/h

**Greek symbols**

µf: fluid viscosity, Pa.s.

**Subscripts**

acc: acceleration pressure drop, Pa
Cyc,s: solid exit of cyclone.
DR: solid in the reactor above entrance of the loop seal
f: fluid.
(f-i)g: Contraction Pressure Drop, Pa
(f-i)p: Acceleration of Solids Pressure Drop, Pa
(f-i)p: Barrel Friction Pressure Drop, Pa
HC: Horizontal conveying line.
L: lift.
ls: loop seal.
lv,v: standpipe of the l-valve.
o: Outlet Exit Contraction in cyclone.
piping: the discharge line of cyclone to atmosphere
rg: Gas Reversal.
r: relative.

δ: gas fraction ratio in the l-valve.
ε: voidage of the bed.
ρ: density, kg/m$^3$.
ϕ: Sphericity of solid particles
s: solid particles.
Tb: Blinded tee bend

## REFERENCES


(1) Lyngfelt Anders, Thunman Hilmer, In: Thomas D.C., Benson S.M., editors. Carbon Dioxide Capture for Storage in Deep Geologic Formations. Elsevier Ltd.; 2005. p. 625-45.
(2) Ryu H.J., Jin G.T., Yi C.K., In: Morris T., Gale J., Thambimuthu K., editors. Elsevier Ltd.; 2005. p. 1907-10.
(3) Shen Laihong, Wu Jiahua, Gao Zhengping, Xiao Jun, Combustion and Flame 2009.
(4) Pröll T., Rupanovits K., Kolbitsch P., Bolhàr-Nordenkampf J., Hofbauer H., Chem Eng Technol 2009;32(3):418-27.
(5) Kronberger Bernhard, Lyngfelt Anders, Lo1 ffler Gerhard, Hofbauer Hermann, Ind Eng Chem Res 2005;44,546-56.
(6) Forero C.R., Gayán P., de Diego L.F., Abad A, García-Labiano F., Adánez J. , Fuel Processing Technology 2009;90(12):1471-779.
(7) de Diego L.F., García-Labiano F., Gayan P., Celaya J., Palacios J.M., Adanez J., Fuel 2007;86:1036-45.
(8) Kolbitsch P., Pröll T., Bolhar-Nordenkampf J., Hofbauer H., Chem Eng Technol 2009;32(3):398-403.
(9) Kronberger B., Johansson E., Löffler G., Mattisson T., Lyngfelt A., Hofbauer H., Chemical Engineering & Technology 2004;27(12):1318-26.
(10) Real Son Sung, Kim Sang Done, Lee Jea-Keun, Vancouver, Canada 2007.
(11) Andrus H.E., Chiu J.H., Thibeault P.R., Brautsch A., Technology Development. 2009.
(12) Noorman S., van Sint Annaland M., Kuipers H., Ind Eng Chem Res 2009;46(12):4212-20.
(13) Noorman S. van Sint Annaland M., Kuipers J.A.M., Chemical Engineering Science 65 (2010) 92 -- 97 .
(14) Dahl Ivar M., Bakken Egil, Larring Yngve, Spjelkavik Aud I., Håkonsen Silje Fosse, Blom Richard, Energy Procedia 2009;1:1513-9.
(15) Gauthier T., Bayle J., Leroy P., Oil & Gas Science and Technology - Rev IFP 2000;55(2):187-207.
(16) Knowlton T.M., Hirsan I. Solids Flow Control using a Nonmechanical L-valve. 1997.
(17) Luckos A., den Hoed P., South African Institute of Mining and Metallurgy; 2005 p. 345-55.
(18) Geldart D, Jones P., Powder Technology 1991;67:163.
(19) Handbook of fluidizfition and fluid-particle systems. New York: Marcel Dekker, Inc.; 2003.
(20) Kunii Daizo, Levenspiel Octave. Fluidization Engineering. 2nd ed. Boston: Butterworth-Heinemann; 1991.
(21) Konno H., Saito S.J., Chem Eng Japan 1969;2:211.
(22) Knowlton K. Cyclone Separators. In: Yang Wen-Ching, editor. Handbook of fluidization and fluid-particle systems.New York: Marcel Dekker; 2003.


.